Data fusion of target characteristic in multistatic passive radar

CAO Xiaomao[1], YI Jianxin[1,*], GONG Ziping[1], RAO Yunhua[1,2], and WAN Xianrong[1,*]

1. School of Electronic Information, Wuhan University, Wuhan 430072, China;
2. Shenzhen Research Institute, Wuhan University, Shenzhen 518057, China

Abstract: Radar cross section (RCS) is an important attribute of radar targets and has been widely used in automatic target recognition (ATR). In a passive radar, only the RCS multiplied by a coefficient is available due to the unknown transmitting parameters. For different transmitter-receiver (bistatic) pairs, the coefficients are different. Thus, the recovered RCS in different transmitter-receiver (bistatic) pairs cannot be fused for further use. In this paper, we propose a quantity named quasi-echo-power (QEP) as well as a method for eliminating differences of this quantity among different transmitter-receiver (bistatic) pairs. The QEP is defined as the target echo power after being compensated for distance and pattern propagation factor. The proposed method estimates the station difference coefficients (SDCs) of transmitter-receiver (bistatic) pairs relative to the reference transmitter-receiver (bistatic) pair first. Then, it compensates the QEP and gets the compensated QEP. The compensated QEP possesses a linear relationship with the target RCS. Statistical analyses on the simulated and real-life QEP data show that the proposed method can effectively estimate the SDC between different stations, and the compensated QEP from different receiving stations has the same distribution characteristics for the same target.

Keywords: data fusion, multistatic passive radar, radar cross section (RCS), target characteristic.

1. Introduction

Automatic target recognition (ATR) is an important part of modern radars. And radar cross section (RCS), which contains abundant target information, is a fundamental and important attribute of targets and is widely studied in the field of ATR [1−5]. Generally, measuring target RCS in an anechoic chamber [6,7] or in a standard testing field [8] with dedicated equipment is the most accurate way. However, if the anechoic chamber or targets are unavailable, those accurate measurement methods will fail

to work.

In practice, for active radars, target RCS can be derived from the radar equation [9−11]. On the contrast, it is almost impossible to obtain target RCS from the radar equation in a passive radar due to the unknown transmitting parameters. Aiming at this problem, a method using signals from the reference channel to help extract RCS from target echo power was proposed in [12]. It introduces direct path signals to help cancel out transmitting parameters and obtains a recovered RCS which is the true RCS with an unknown parameter. For a single transmitter-receiver (bistatic) pair, the parameter is almost constant for all detected targets and would not affect the target characteristics.

However, in a real situation, it is hard to collect enough and comprehensive data by a passive radar with only one transmitter-receiver (bistatic) pair for analyzing target characteristics and training a good classifier for ATR. For one thing, for such a fixed passive radar, it is time-consuming to collect enough target data by only one receiving station due to its limited observation area. For another, for civil aviation aircraft, the flight paths of the aircraft change very little within a certain airspace, thus the radar's observation angle to the target is limited and target information collected by the radar is incomplete. Thus, we hope to use multiple receiving stations to simultaneously observe the target at different angles so as to improve the efficiency of data collection as well as obtain comprehensive target information. Each receiving station can form a transmitter-receiver (bistatic) pair with the transmitting station. However, as the parameter settings of different transmitter-receiver (bistatic) pairs are not exactly the same, the unknown coefficient in the recovered RCS varies with different receiving stations. Thus, the recovered RCS from different receiving stations is incomparable and cannot be fused. To the best of our knowledge, there have been no literature reporting on data fusion for target characteristics analysis in multistatic passive radars yet.

To tackle the aforementioned problem, in this paper we

propose a quantity named the quasi-echo-power (QEP) as well as a method for eliminating differences of this quantity among different transmitter-receiver (bistatic) pairs. The relationship between the QEP compensated for station difference and RCS is a simple linear relationship. Thus, it is the same to analyze target characteristics using the compensated QEP as using RCS. The compensated QEP overcomes the problem that the recovered RCS in different transmitter-receiver (bistatic) pairs is not comparable, which makes it possible to fuse data from different receiving stations for target characteristics analysis and further use in ATR.

The remainder of this paper is organized as follows. Section 2 presents the formulation of station difference coefficient (SDC) and QEP. Section 3 shows the simulation results of SDC estimation and statistical analysis of distribution characteristics of QEP. Section 4 uses experimental data to validate the effectiveness of the proposed QEP as well as the method of eliminating station difference in a real situation. Conclusions are drawn in Section 5.

2. Formulation of SDC and QEP

For a single transmitter-receiver (bistatic) pair, the classical bistatic radar equation is defined as follows [13]:

$$P_r = \frac{P_t G_t F_t^2(\theta_t,\varphi_t) G_r F_r^2(\theta_r,\varphi_r)\lambda^2\sigma}{(4\pi)^3 R_t^2 R_r^2} \tag{1}$$

where P_r is the received echo power of the target; P_t is the transmitting power of the signal; G_t is the gain of the transmitting end; $F_t(\theta_t,\varphi_t)$ is the pattern propagation factor for the transmitter-to-target path; θ_t and φ_t are the two components of the angle between the transmitter-to-target line and the normal direction of the transmitting antenna; G_r is the gain of the receiving end; $F_r(\theta_r,\varphi_r)$ is the pattern propagation factor for the receiver-to-target path; θ_r and φ_r are the two components of the angle between the receiver-to-target line and the normal direction of the receiving antenna; λ is the wavelength; σ is the bistatic RCS (BRCS); R_t is the transmitter-to-target range; and R_r is the receiver-to-target range.

In a real situation, the transmitting antenna is often omnidirectional in the azimuth plane and the antenna beam in the vertical plane is able to cover targets in low altitudes. Thus, the pattern propagation factor for the transmitter-to-target path can be taken as an angle-independent variable, i.e., $F_t(\theta_t,\varphi_t) = 1$. Meanwhile, the pattern propagation factor for the receiver-to-target path is known to us. Thus, $F_r(\theta_r,\varphi_r)$ can be compensated. Under this assumption, (1) can be rewritten as follows:

$$P_r' = \frac{P_r}{F_r^2(\theta_r,\varphi_r)} = \frac{P_t G_t G_r \lambda^2\sigma}{(4\pi)^3 R_t^2 R_r^2} \tag{2}$$

where P_r' denotes the target echo power that is compensated for the pattern propagation factor for the receiver-to-target path. Pick out and denote parameters related to receiving and transmitting as a coefficient k, then we have k as follows:

$$k = \frac{P_t G_t G_r \lambda^2}{(4\pi)^3}. \tag{3}$$

For a certain transmitter-receiver (bistatic) pair, this k parameter is a constant and we call it the constant of the transmitter-receiver (bistatic) pair. With this constant, we can find out the difference of parameter settings between different transmitter-receiver (bistatic) pairs so as to compensate target echo power in different receiving stations to the same power level.

Assume there is a multistatic passive radar with one transmitter, which is denoted as T_x, and two receivers, which are denoted as R_{xi} and R_{xj}. The two receivers operate on the same frequency and polarization state. Denote the transmitter-receiver (bistatic) pair composed of R_{xi} and T_x as transmitter-receiver (bistatic) pair i, whose constant of the transmitter-receiver (bistatic) pair is k_i, the transmitter-receiver (bistatic) pair composed of R_{xj} and T_x as transmitter-receiver (bistatic) pair j, whose constant of the transmitter-receiver (bistatic) pair is k_j, and choose R_{xj} as the reference receiving station. And assume there is a target whose BRCS under incident angle of (θ_i,φ_i) and observation angle of (θ_s,φ_s) is σ. This target is moving in the detection area of the radar. At two different moments of t_i and t_j, the two receiving stations receive two target echo powers, i.e., P_{ri} and P_{rj}, under the same incident angle (θ_i,φ_i) and observation angle (θ_s,φ_s), as shown in Fig. 1. The incident angle (θ_i,φ_i) and observation angle (θ_s,φ_s) are defined in the target coordinate system, and the coordinates of the two positions, i.e., (x_{ti},y_{ti},z_{ti}) and (x_{tj},y_{tj},z_{tj}), corresponding to t_i and t_j are defined in the radar coordinate system. It should be noted that (x_{ti},y_{ti},z_{ti}) and (x_{tj},y_{tj},z_{tj}) are not necessarily two points in a same track, but the (θ_i,φ_i) and (θ_s,φ_s) at these two positions are the same. And since the BRCS of a target is only related to its own characteristics as well as the frequency, wave form, and polarization state of the incident electromagnetic wave but has nothing to do with other factors such as the observation time, the target BRCSs observed by the two receiving stations at t_i and t_j are equal, i.e., $\sigma_i = \sigma_j = \sigma$. For R_{xi}, the target comes from angle of $(\theta_{ri},\varphi_{ri})$ in the radar coordinate system with R_{xi} as the origin. For R_{xj}, the target comes from angle of $(\theta_{rj},\varphi_{rj})$ in the radar coordinate system with R_{xj} as the origin.
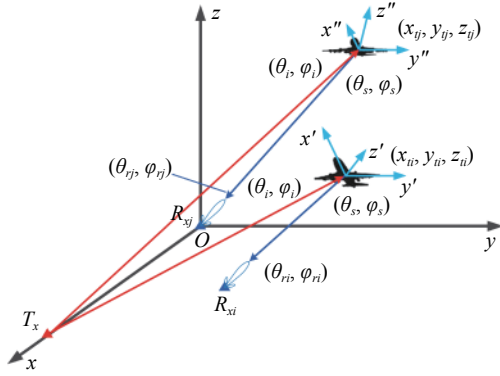
Fig. 1 **Sketch map of the relationship between the multistatic radar and the target**

Then we have two relationships of the target echo power and the BRCS according to (2), i.e.,

$$\begin{cases} P'_{ri} = \dfrac{P_{ri}}{F_{ri}^2(\theta_{ri}, \varphi_{ri})} = \dfrac{k_i\sigma_i}{R_{ti}^2 R_{ri}^2} \\ P'_{rj} = \dfrac{P_{rj}}{F_{rj}^2(\theta_{rj}, \varphi_{rj})} = \dfrac{k_j\sigma_j}{R_{tj}^2 R_{rj}^2} \end{cases}. \quad (4)$$

As mentioned before, we have $\sigma_i = \sigma_j = \sigma$. Thus, we can obtain the following relationship between k_i and k_j according to (4) as

$$\alpha_{ij} \triangleq \frac{k_i}{k_j} = \frac{P_{ri}F_{rj}^2(\theta_{rj}, \varphi_{rj})R_{ti}^2 R_{ri}^2}{P_{rj}F_{ri}^2(\theta_{ri}, \varphi_{ri})R_{tj}^2 R_{rj}^2} \quad (5)$$

where α_{ij} is defined as the SDC of k_i relative to k_j. Meanwhile, we also have α_{ij} from (3) as follows:

$$\alpha_{ij} = \frac{P_{ti}G_{ti}G_{ri}}{P_{tj}G_{tj}G_{rj}}. \quad (6)$$

Equation (6) is the definition formula whereas (5) is for calculation. Then, divide P'_{ri} in (4) by α_{ij} and compensate both P'_{ri} and P'_{rj} for distance and denote the compensated target echo power as $\bar{P}_{ri}$ and $\bar{P}_{rj}$, respectively. We call $\bar{P}_{rj}$ QEP and $\bar{P}_{ri}$ the compensated QEP. In other words, the QEP is the target echo power only compensated for the pattern propagation factor and distance, whereas the compensated QEP is the one also compensated for station difference. Then we have

$$\begin{cases} \bar{P}_{ri} = \dfrac{P_{ri}R_{ti}^2 R_{ri}^2}{\alpha_{ij}F_{ri}^2(\theta_{ri}, \varphi_{ri})} = k_j\sigma_i \\ \bar{P}_{rj} = \dfrac{P_{rj}R_{tj}^2 R_{rj}^2}{F_{rj}^2(\theta_{rj}, \varphi_{rj})} = k_j\sigma_j \end{cases}. \quad (7)$$

Since $\sigma_i = \sigma_j$, as mentioned before, we have $\bar{P}_{ri} = \bar{P}_{rj}$. Moreover, if $\sigma_i \neq \sigma_j$, then $\bar{P}_{ri} \neq \bar{P}_{rj}$. In this case, the difference between $\bar{P}_{ri}$ and $\bar{P}_{rj}$ only comes from target RCS but not from the parameter setting of the two transmitter-receiver (bistatic) pairs, which makes the compensated

QEP in R_{xi} equivalent to be in the same station as the QEP in R_{xj}. Since the SDC of the reference receiving station relative to itself is 1, the QEP in the reference receiving station can also be seen as the compensated QEP. Thus, data in the two stations become comparable and can be fused for the analysis of target characteristics. Moreover, the compensated QEP has a linear relationship with BRCS, which means the compensated QEP is also equivalent to a quasi-BRCS. Thus, we are able to know the characteristics of a target's BRCS by analyzing the compensated QEP.

3. Simulation results

3.1 Estimation of SDC

There are three targets used in the simulation, namely Cessna 172, Airbus 320, and Boeing 747, as shown in Fig. 2(a), Fig. 2(b), and Fig. 2(c). For each target, we randomly generate 1 000 tracks and pick 953 tracks that are in the area of interest. The length of each track is 20 points. The start points of these tracks are uniformly distributed in the area of interest while their orientations conform to the uniform distribution in $[0, 2\pi]$. We set the target speed to 200 m/s for all three targets. The simulation scenario is shown in Fig. 2(d), where the black parallelogram whose size is 8 km×8 km denotes the given area for target moving; the red triangle marked with T_x is the simulated transmitting station; the three blue triangles marked with R_{x1}, R_{x2} and R_{x3} are the three simulated receiving stations. Their receiving gain are set to be 10 dB, 15 dB, and 20 dB, respectively. Thus, the true values of SDCs of R_{x2} and R_{x3} relative to R_{x1} can be obtained according to (6), which are 3.16 and 10. The array antenna used in the three receiving stations are all set to be uniform linear array but with 5 elements, 7 elements, and 11 elements respectively. It should be noted that the location coordinates of the three receiving stations and the height of the given area are not shown in true proportions in order to show their relationship clearly. At the meantime, the BRCS database of the three targets is calculated by the commercial software High Frequency Structure Simulator (HFSS) at a frequency of 546 MHz. Then, the incident angle and the scattering angle of the electromagnetic wave in the target coordinate system corresponding to each point on the track are estimated according to the target position, the station layout of transmitting station, and the receiving station and the target attitude which is estimated according to the method proposed in [14]. Using the estimated angles, we extract BRCS for each point on the track from the aforementioned BRCS database. Then, we generate the simulated target echo power for each track. Without loss of generality, assume all echo

power data are received with an array pattern formed at the azimuth angle of 45°. The array patterns for the three

receiving stations are shown in Fig. 2(e).

(a) Cessna 172

(b) Airbus 320

(c) Boeing 747

(d) Simulated scenario

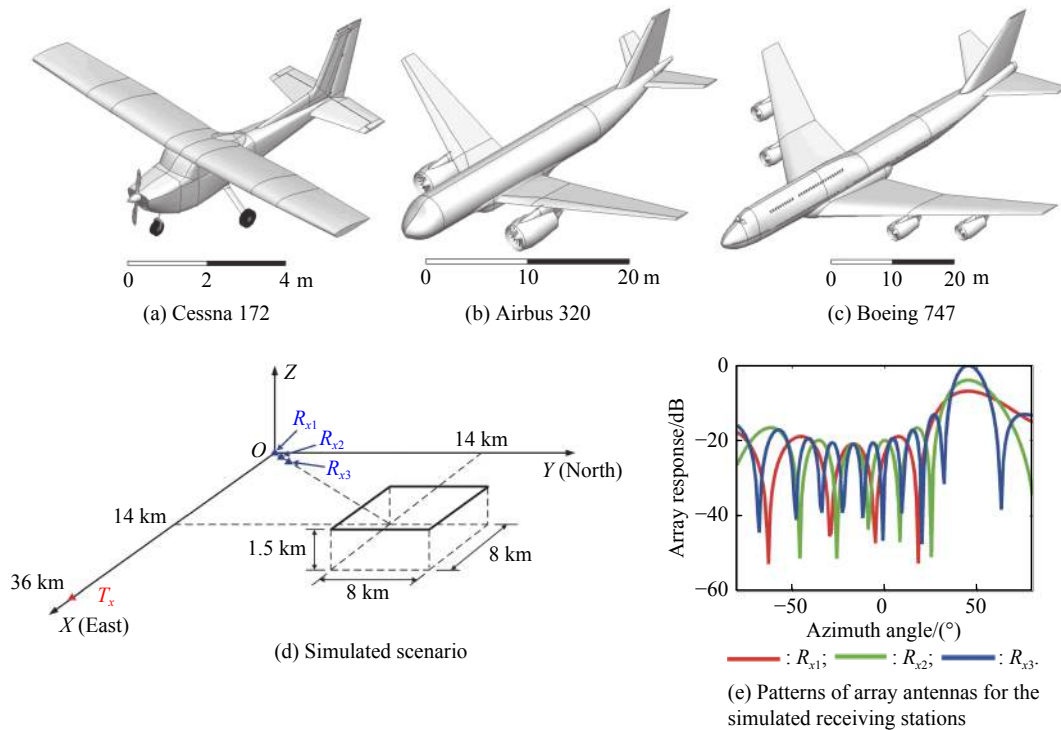(e) Patterns of array antennas for the simulated receiving stations

Fig. 2   Configuration for simulation

We choose R_{x1} as the reference receiving station and then estimate SDCs of R_{x2} and R_{x3} relative to R_{x1} according to (5). It should be noted that when matching the incident angles and observation angles of two sets of data, we do not require the corresponding angles to be exactly equal in value, but when their difference is less than a threshold, they are considered to be equal. In this paper, the threshold of angle difference is set to 1° in consideration of the limited angle measurement accuracy of real-life radars. In a real situation, influences from noise and fluctuation of BRCS on the target echo power are inevitable, which would lead to estimation error of SDC. Two

simple and intuitive ways to reduce the estimation error are to average multiple measurements and to increase the signal-to-noise ratio (SNR). Due to the angle matching strategy used, it is required that the target echo power should be slowly fluctuating with the attitude angle, in order to employ the method of averaging multiple measurements to reduce the estimation error of SDC. Thus, in the SDC estimation, it is required to use targets of Swerling I and Swerling III. We generate multiple sets of target echo power with different SNRs. The SNR ranges from 5 dB to 50 dB with a step of 5 dB. The estimated SDCs for R_{x2} and R_{x3} are shown in Fig. 3 and Fig. 4, respectively.
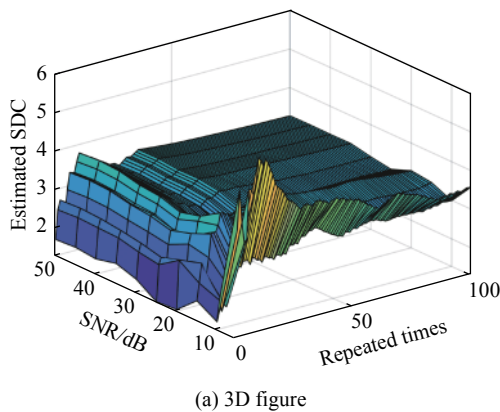
(a) 3D figure
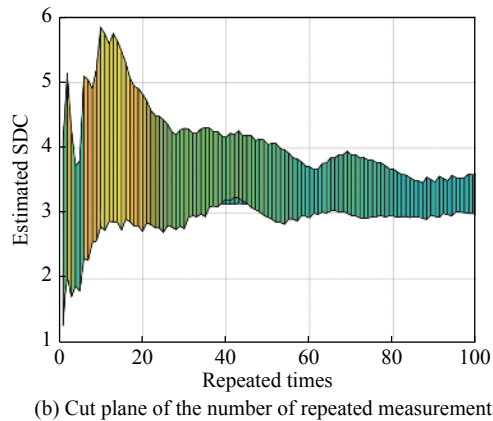
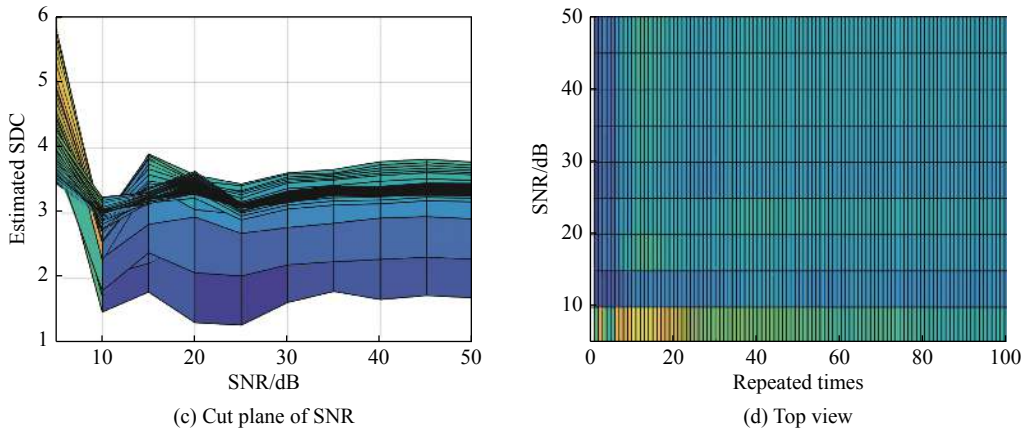(b) Cut plane of the number of repeated measurements

(c) Cut plane of SNR

(d) Top view

Fig. 3   SDC estimation of R_{x2}

(a) 3D figure

(b) Cut plane of the number of repeated measurements
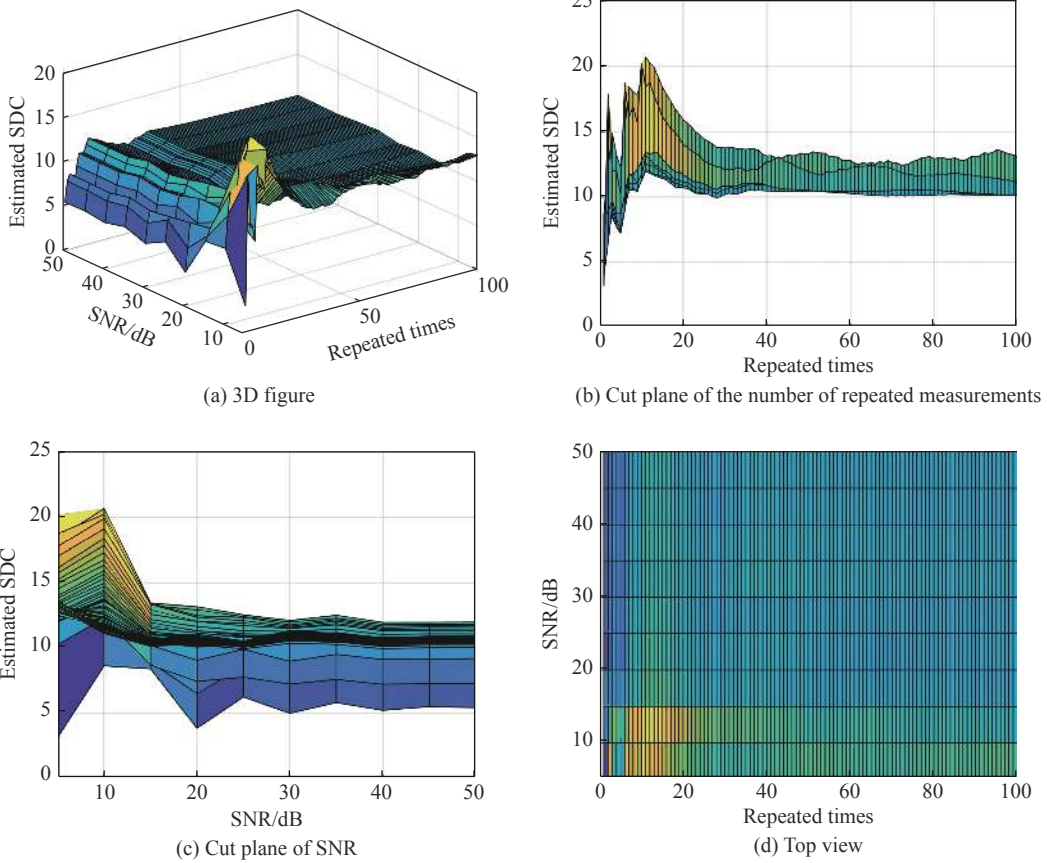
(c) Cut plane of SNR

(d) Top view

Fig. 4   SDC estimation of R_{x3}

In Fig.3, the true value is 3.16; the black part in Fig.3(c) denotes that there are many curves gathering around the same value, which means the estimation converges to that value.

In Fig. 4, the true value is 10, and the black part in Fig. 4(c) denotes that there are many curves gathering around the same value, which means the estimation converges to that value.

It can be seen from Fig. 3(d) that when SNR > 30 dB and the number of repeated measurements is greater than 35, the estimated value of the SDC becomes stable. This result indicates that the SDC converges to the true value when SNR and the number of repeated measurements increase. In particular, SDC of R_{x2} converges to 3−3.5 with the number of repeated measurements increasing, as shown in Fig. 3(b). At the meantime, when the number of repeated measurements for average reaches a certain amount, the SDC of R_{x2} would also converge to 3−3.5 with the SNR increasing. As shown in Fig. 3(c), the estimation curves concentrate on around the value of 3,

which indicates that most of the estimations are close to 3. The same variation trend and conclusion are also applied to the SDC estimation of R_{x3}, as shown in Fig. 4. What is different is that the SDC estimate of R_{x3} converges to about 10.

3.2 Analysis of distribution characteristics of QEP

In this section, we choose simulated target data whose SNR = 30 dB to estimate the SDC for the reason that this SNR is in accordance with the real situation in our passive radar system. Fig. 5 shows the SDC estimates of R_{x2} and R_{x3} between different SNRs when the number of repeated measurements is 100. It can be seen from Fig. 5 that when SNR = 30 dB, SDC estimates for R_{x2} and R_{x3} are 3.16 and 10.55, respectively. Compared to the values we set in the simulation, which are 3.16 and 10, the percentage errors are 0.00% and 5.50%, respectively. Using these two SDCs, we compensate the simulated QEP and get the compensated QEP data. For each track, we have a time sequence of the QEP. For each sequence, we calculate three features, i.e., the minimum value, the median value, and the maximum value. The following statistical analysis is made based on the tracks corresponding to angle ranges of $90° \leqslant \theta_i \leqslant 120°$, $0° \leqslant \varphi_i \leqslant 30°$, $90° \leqslant \theta_s \leqslant 120°$, $90° \leqslant \varphi_s \leqslant 120°$ in the target coordinate system.
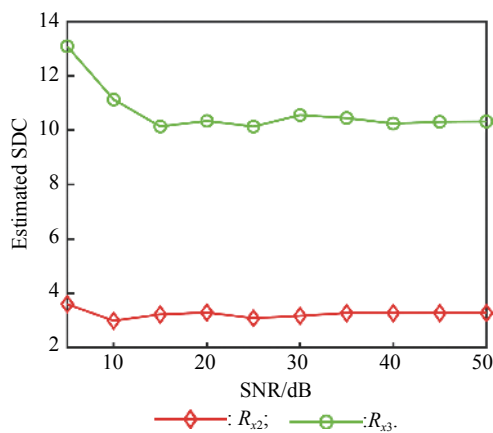

Fig. 5   SDC estimates of R_{x2} and R_{x3} between different SNRs when the number of repeated measurements is 100

(i) Comparison of characteristics of QEP among different stations

We take Cessna 172 as an example to investigate the distribution characteristics of each QEP feature of the target in different receiving stations, as shown in Fig. 6. It should be noticed that to conveniently make comparisons, we take the amplitude of the histogram, connect it into a broken line, and express the histogram into a broken line graph. The upper figures in Fig. 6 are results with compensation only for distance and the pattern propagation

factor for the receiver-to-target path whereas the lower figures are results with compensation also for the station difference. It can be seen from figures on the upper row in Fig. 6 that the distributions of the features in different receiving stations are quite different from each other before compensation for station difference. Not only do the peak locations of the distribution curves from different receiving stations differ from each other, but also their abscissa ranges differ. However, after compensation for the station difference, distribution curves for the same feature almost coincide with each other, as shown in Fig. 6(d), Fig. 6(e), and Fig. 6(f). These results indicate that the compensated QEP from different receiving stations are comparable and can be fused. We can also see from Fig. 6(d), Fig. 6(e), and Fig. 6(f) that distribution curves of the same feature from different receiving stations are not exactly the same, even if they are compensated for the station difference. The reason about this is that the amount of tracks used to make statistical analysis in each receiving station is not equal. Since the distribution of occurrence rate is an approximation of the probability distribution, the unequal amount of data used to make statistical analysis will lead to differences in the distribution of the occurrence rate.

(ii) Comparison of characteristics of QEP among different targets

In this section, we discuss the influence of the station difference on target characteristics and show the necessity to compensate for the station difference in order to obtain correct characteristics of the targets from the fused data. We fuse target data from different receiving stations by packing them according to the target type. Both the data with and without compensation for the station difference are fused in order to make comparison. Results of statistical analysis are shown in Fig. 7. It can be seen from Fig. 7(d) that the right end of the distribution curve of Cessna 172 after compensation is only about 25 dB, whereas the right end of the one before compensation is extended to about 40 dB, as shown in Fig. 7(a). The main reason for this is that the value range of the QEP before compensation is extended by the SDC. The extension of the QEP value range could cause the values not belonging to Cessna 172 to be mistakenly classified as Cessna 172's. And just because of the extension of the value range, the distribution histogram of the occurrence rate is changed and deviates from the true target characteristics. As shown in Fig. 7(a) and Fig. 7(d), the distribution before compensation differs a lot from the one after compensation. The aforementioned phenomenon and analysis coming from the distribution characteristics of the minimum value are also applied to the other two features. These results demonstrate that compensation for the station difference is necessary to obtain the correct target characteristics.
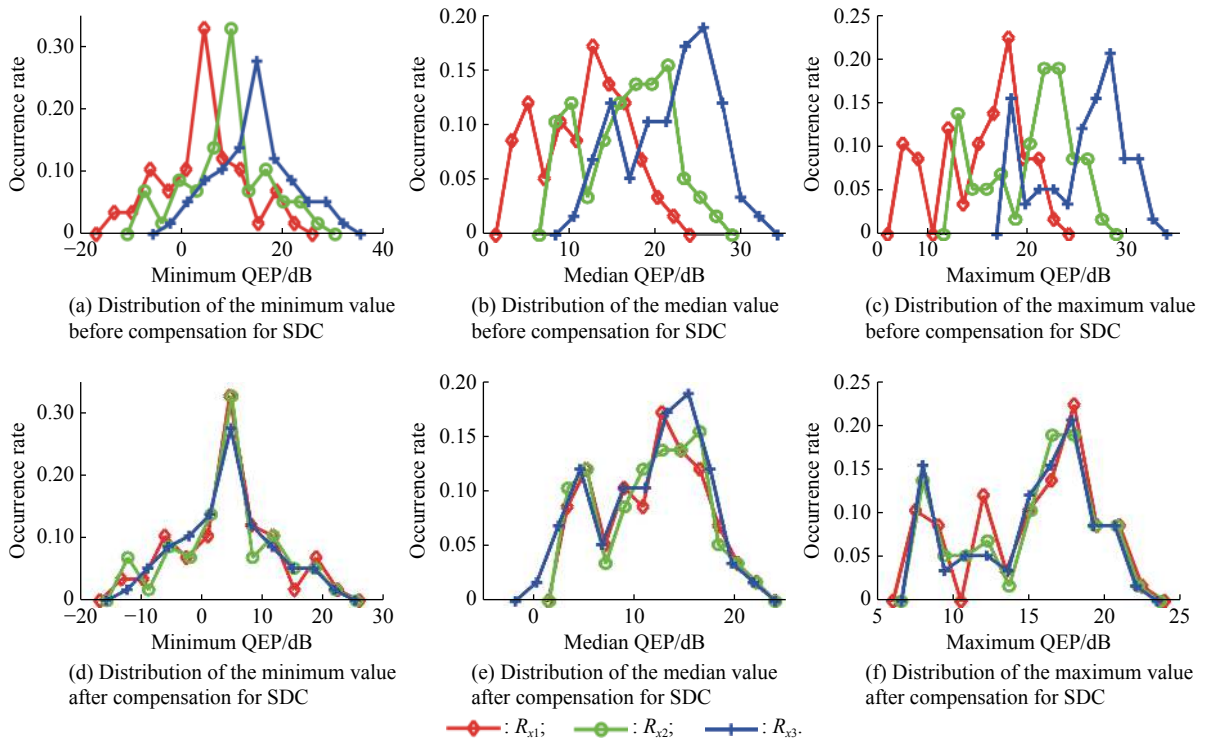
(a) Distribution of the minimum value
before compensation for SDC

(b) Distribution of the median value
before compensation for SDC

(c) Distribution of the maximum value
before compensation for SDC

(d) Distribution of the minimum value
after compensation for SDC

(e) Distribution of the median value
after compensation for SDC

(f) Distribution of the maximum value
after compensation for SDC

—◇— : R_{x1}; —○— : R_{x2}; —+— : R_{x3}.

Fig. 6   Occurrence rate distribution histogram of Cessna 172's three features from three simulated receiving stations

(a) Distribution of the minimum value
before compensation for SDC

(b) Distribution of the median value
before compensation for SDC

(c) Distribution of the maximum value
before compensation for SDC

(d) Distribution of the minimum value
after compensation for SDC

(e) Distribution of the median value
after compensation for SDC

(f) Distribution of the maximum value
after compensation for SDC

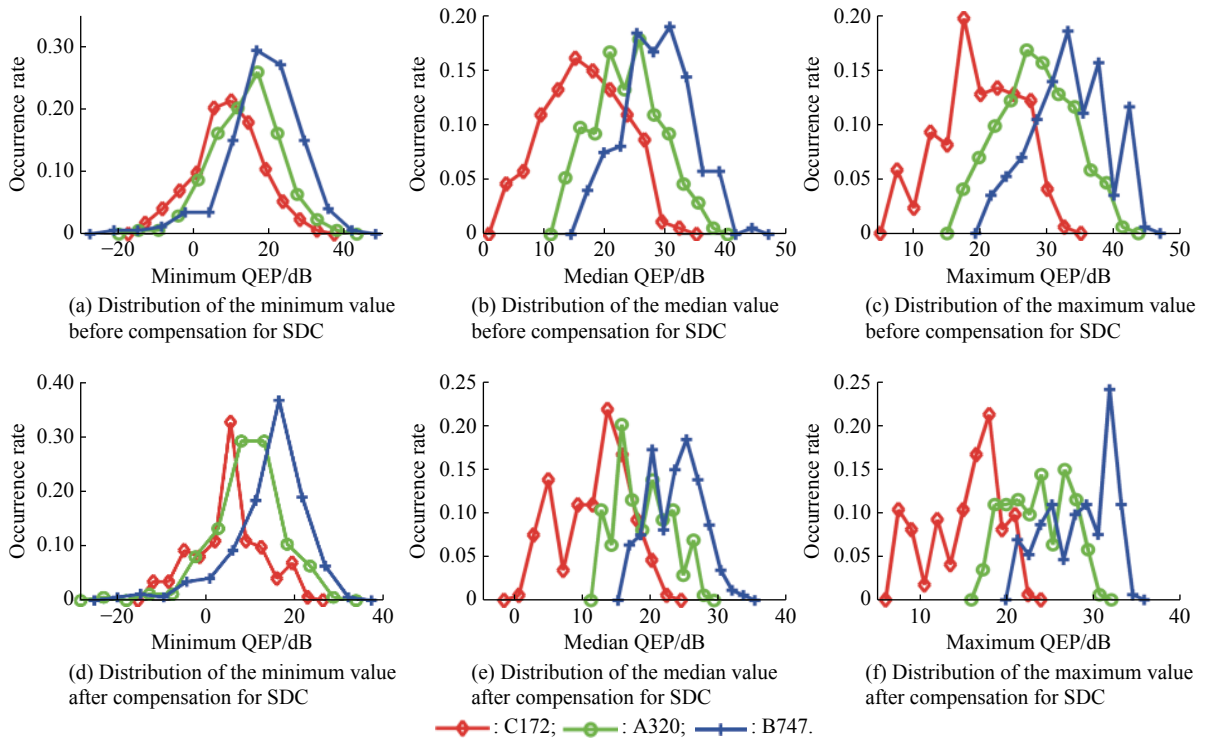—◇— : C172; —○— : A320; —+— : B747.

Fig. 7   Occurrence rate distribution histogram of three features from three different simulated targets

4. Experiment results

Experimental data are collected in Luoyang Beijiao Airport with multistatic passive radar developed in Wuhan University, whose configuration is shown in Fig. 8(a).

The multistatic passive radar consists of one transmitter and two receivers, namely R_{x1} and R_{x2}. Two receiving antenna arrays directing to different directions are used to collect abundant information of airplanes. Information of

cooperative targets, which are SR20 and MA600, are obtained and confirmed by the automatic dependent surveillance broadcast (ADS-B), as shown in Fig. 8(b) and Fig. 8(c). It should be noted that SR20 is a small plane whose size is smaller than that of MA600. High-precision tracks with target echo power are obtained by using methods proposed in [15].
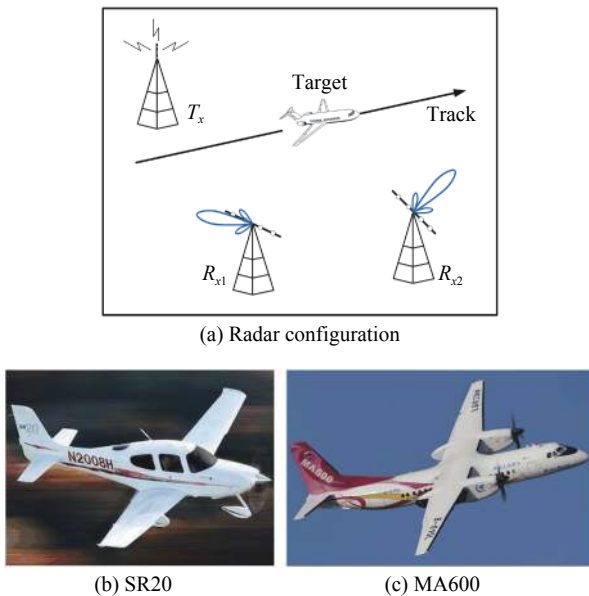

(a) Radar configuration

(b) SR20   (c) MA600

Fig. 8   **Configuration of the multistatic passive radar and the cooperative targets**

Before conducting ATR with the output data, preprocessing including eliminating the station difference of data from different receiving stations is required so as to obtain correct target distribution characteristics from statistical analysis. We choose R_{x1} as the reference station and estimate the SDC of R_{x2} relative to R_{x1}. Result of the SDC estimation is shown in Fig. 9.
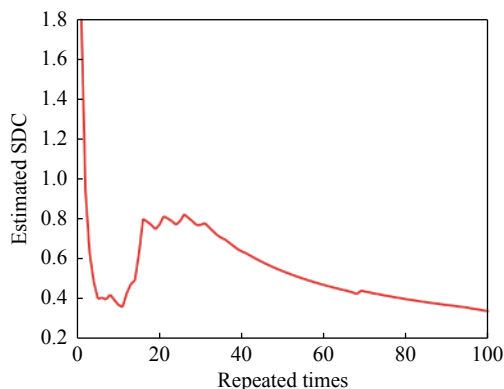

Fig. 9   Estimated SDC of R_{x2}

The horizontal axis in Fig. 9 denotes the number of repeated measurements of SDC. As can be seen from Fig. 9, with the number of repeated measurements increasing, the value of the estimated SDC tends to be stable, which means the estimation is convergent and validates the use of averaging on repeated measurements in SDC estimation. Thus, we choose the value after an average of 100 times as the final estimation of R_{x2}'s SDC, which is 0.34.

We compensate target echo power from R_{x2} for station difference using the aforementioned SDC estimate. Meanwhile, target echo power from R_{x2} and R_{x1} are both compensated for distance and pattern propagation factor for the target-to-receiver path. In this way, we obtain the corresponding compensated QEP. To validate the SDC estimate of R_{x2}, a comparison between the target distribution characteristics of SR20 obtained from the data before compensation for SDC and those obtained from the data after compensation for SDC is made in Fig. 10. It should be noted that the following statistical analysis is made based on tracks corresponding to the angle range of $90° \leqslant \theta_i \leqslant 120°, 0° \leqslant \varphi_i \leqslant 30°, 120° \leqslant \theta_s \leqslant 150°, 210° \leqslant \varphi_s \leqslant 240°$ in the target coordinate system.

It can be seen from Fig. 10 that distribution curves of the same target in different receiving stations differ from each other. Difference of the curve shape comes from different amounts of data. Since these curves are approximations of the probability distribution function and the amount of data used in analysis would affect the curve shape, the difference in the curve shape is reasonable and acceptable in consideration of the similar change trend of these curves. However, difference in abscissa ranges of the curve should be eliminated since it comes from the station difference. This difference will lead to obtaining wrong distribution characteristics of the fused data. As shown in the upper row of Fig. 10, there is a deviation for the green curve from the red curve which is the reference curve. After compensation for station difference using SDC, this deviation is offset, as shown in the lower row of Fig. 10. Results shown in Fig. 10 validate the correctness of the estimated SDC.

A further comparison between target distribution characteristics obtained from fused target data before compensating the station difference and those obtained from fused target data after compensating the station difference is also made in Fig. 11. For one thing, the curve span is reduced after compensation for station difference. Reason for this is that the station difference reflecting on the SDC makes the QEP level in R_{x2} lower than that in R_{x1}. Thus, the value range of QEP is extended on the lower boundary after data fusion, making the curve span before compensation wider than that after compensation. For another, an obvious change in the curve shape is observed from the comparison. As shown in Fig. 11(c) and Fig. 11(f), position of the curve peak of MA600 changes from around 180 dB to larger than 200 dB. If we consider this

peak location as an identifying feature, the difference resulted by station difference could lead to very different recognition results. Comparison shown in Fig. 11 demonstrates the necessity to compensate station difference of QEP in target characteristics analysis for multistatic passive radars.
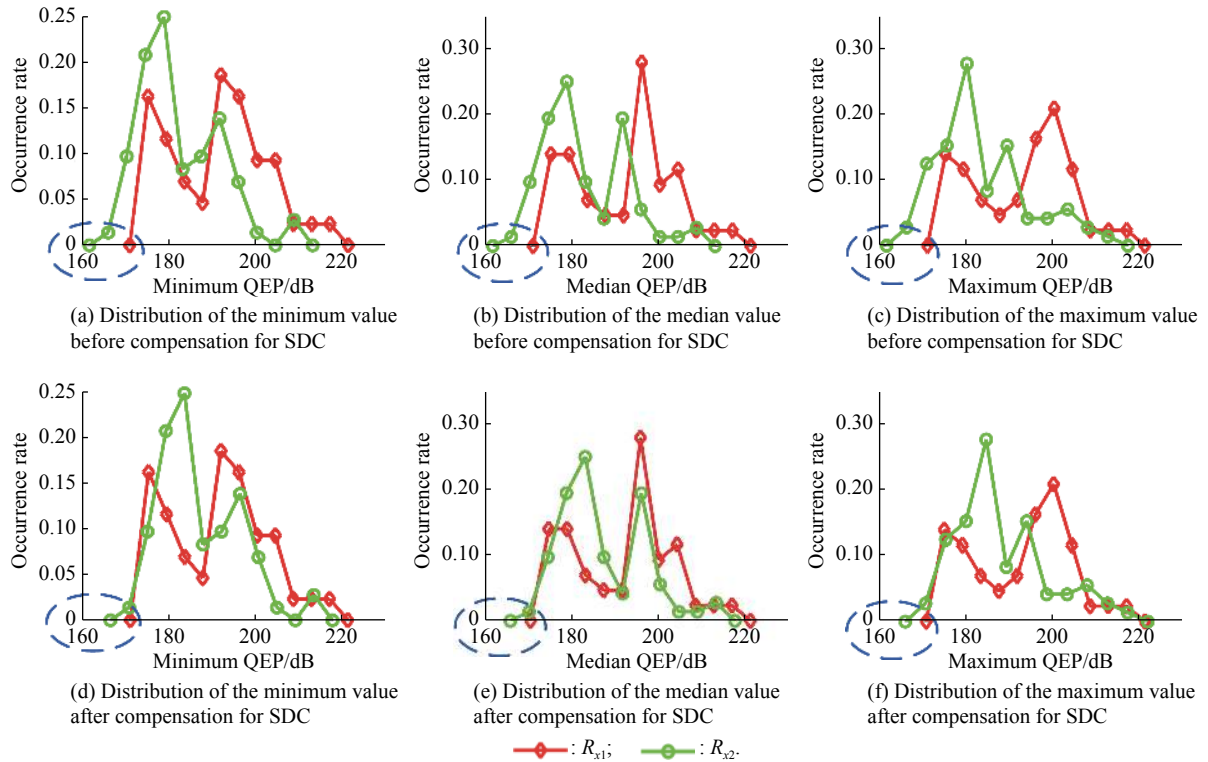

(a) Distribution of the minimum value before compensation for SDC

(b) Distribution of the median value before compensation for SDC

(c) Distribution of the maximum value before compensation for SDC

(d) Distribution of the minimum value after compensation for SDC

(e) Distribution of the median value after compensation for SDC

(f) Distribution of the maximum value after compensation for SDC

◆ : R_{x1};   ○ : R_{x2}.

Fig. 10   Occurrence rate distribution histogram of SR20's three features from two receiving stations

(a) Distribution of the minimum value before compensation for SDC

(b) Distribution of the median value before compensation for SDC

(c) Distribution of the maximum value before compensation for SDC

(d) Distribution of the minimum value after compensation for SDC

(e) Distribution of the median value after compensation for SDC

(f) Distribution of the maximum value after compensation for SDC
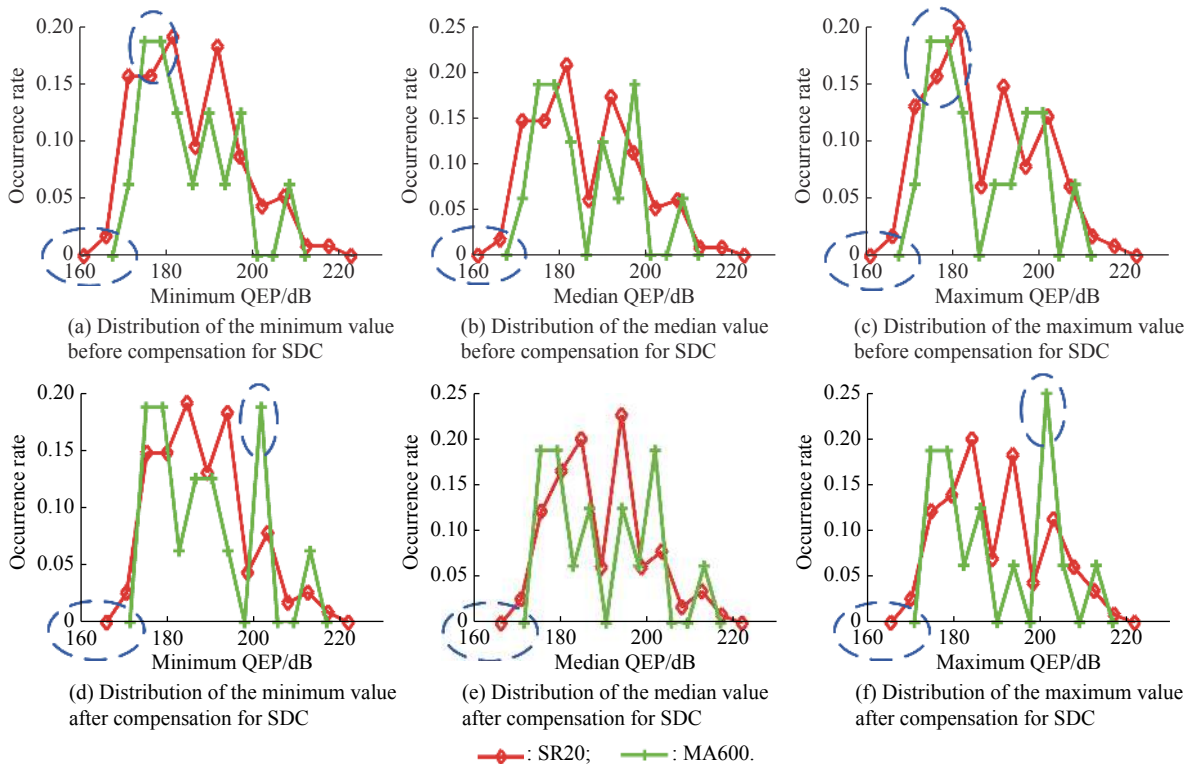
◆ : SR20;   + : MA600.

Fig. 11   Occurrence rate distribution histogram of three features from different measured targets

5. Conclusions

In this paper we propose a method to eliminate the station difference in target echo power for multistatic passive radars. We estimate the SDCs of all receiving stations relative to the reference receiving station and compensate the QEP data with them. Statistical analysis on the simulated and real-life QEP data show that the station difference can be effectively compensated by the estimated SDC, which validates the effectiveness of the proposed method. Moreover, statistical results also demonstrate that the features defined on the time sequence of the compensated QEP possess obvious difference for different targets, which indicates that they are beneficial features to be used in ATR.

References

[1] ZHANG J, HU S L, YANG Q, et al. RCS statistical features and recognition model of air floating corner reflector. Systems Engineering and Electronics, 2019, 41(4): 780–786. (in Chinese)

[2] CHEN Z R, GU H, SU W M, et al. Ground target classification for low resolution radar based on the probability distribution of feature. Systems Engineering and Electronics, 2016, 38(2): 274–280. (in Chinese)

[3] LEE S J, JEONG S J, KANG B S, et al. Classification of shell-shaped targets using RCS and fuzzy classifier. IEEE Trans. on Antennas and Propagation, 2016, 64(4): 1434–1443.

[4] WANG T, BI W J, ZHAO Y L, et al. Target recognition algorithm based on RCS observation sequence-set-valued identification method. Proc. of the 33rd Chinese Control Conference, 2014: 881–886. (in Chinese)

[5] CHENG Q, CHEN L, ZHANG Y L. Classification of RCS sequences based on KL divergence. The Journal of Engineering, 2019, 20: 6475–6478.

[6] PISA S, PIUZZI E, PITTELLA E, et al. Numerical and experimental evaluation of the radar cross section of a drone. Proc. of the 15th European Radar Conference, 2018: 309–312.

[7] COMBLET F. Radar cross section measurements in an anechoic chamber: description of an experimental system and post processing. Proc. of the IEEE Conference on Antenna Measurements & Applications, 2014: 1–4.

[8] ZHANG Z C, LI W C, YUAN X Y, et al. A dynamic measurement method of target's RCS based on measure system on airship. Journal of CARIT, 2015, 10(5): 551–556. (in Chinese)

[9] ZHANG Z D, LI X, ZHANG J P, et al. Dynamic measurement method of target RCS based on attitude correction. Systems Engineering and Electronics, 2019, 41(6): 1242–1248. (in Chinese)

[10] NIAN P L, LIU R F. Research into dynamic measurement method of RCS for small skimming flying targets. Shipboard Electronic Countermeasure, 2019, 42(4): 5–9. (in Chinese)

[11] JIA J P, DUAN Q S. A RCS measurement method for external field radar. Electronic Test, 2019(9): 64, 65, 67. (in Chinese)

[12] PISANE J, AZARIAN S, LESTURGIE M, et al. Automatic real-time collection of RCS of airplanes in a real bistatic low-frequency configuration using a software defined passive radar based on illuminators of opportunity. Proc. of the IEEE Radar Conference, 2012: 950–955.

[13] SKOLNIK M I. Radar handbook. 3rd ed. Beijing: Publishing House of Electronics Industry, 2005. (in Chinese)

[14] Ehrman L M, Lanterman A D. Extended Kalman filter for estimating aircraft orientation from velocity measurements. IET Radar, Sonar & Navigation, 2008, 2(1): 12−16.

[15] SHU K, YI J X, WAN X R, et al. A hybrid tracking algorithm for multistatic passive radar. IEEE Systems Journal, 2020, 15(2): 2024–2034.

Biographies

CAO Xiaomao was born in 1990. He received his B.E. degree in radio wave propagation and antenna from Wuhan University, in which he is pursuing his Ph.D. degree. His research interests are wideband antenna design and automatic target recognition.
E-mail: cao_xm@whu.edu.cn

YI Jianxin was born in 1989. He received his B.E. degree in electrical and electronic engineering, and his Ph.D. degree in radio physics from Wuhan University in 2011 and 2016, respectively. From August 2014 to August 2015, he was a visiting Ph.D. student at the University of Calgary. He is currently an associate professor with the School of Electronic Information, Wuhan University. His main research interests include radar signal processing, target tracking, and information fusion.
E-mail: jxyi@whu.edu.cn

GONG Ziping was born in 1977. He received his B.E. degree and Ph.D. degree in radio physics from Wuhan University in 1999 and 2007 respectively. He is currently a lecturer with the School of Electronic Information, Wuhan University. His research interests include electromagnetic wave propagation, electromagnetic field simulation, and radio ocean remote sensing.
E-mail: zpgong@whu.edu.cn
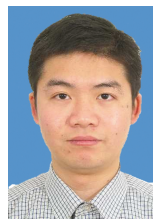
RAO Yunhua was born in 1972. He received his B.E. degree from Harbin Engineering University in 1995, and his Master's degree and Ph.D. degree from Huazhong University of Science and Technology in 2000 and 2004 respectively. He is currently an associate professor with the School of Electronic Information, Wuhan University. His research interests include design of new radar system and wireless communication network.
E-mail: ryh@whu.edu.cn

WAN Xianrong was born in 1975. He received his B.E. degree in electrical and electronic engineering from the former Wuhan Technical University of Surveying and Mapping in 1997, and his Ph.D. degree in radio physics from Wuhan University in 2005. He is currently a professor and a Ph.D. candidate supervisor with the School of Electronic Information, Wuhan University. He hosted and participated in more than 10 national research projects and published more than 80 academic papers. His main research interests include design of new radar systems such as passive radars and over-the-horizon radars, and array signal processing.
E-mail: xrwan@whu.edu.cn